



ELSEVIER

February 2002

Materials Letters 52 (2002) 304–312

**MATERIALS  
LETTERS**

www.elsevier.com/locate/matlet

# Comparative study on phase development of lead titanate powders

Jiye Fang<sup>a,\*</sup>, John Wang<sup>a</sup>, Leong-Ming Gan<sup>b</sup>, Ser-Choon Ng<sup>c</sup><sup>a</sup> Department of Materials Science, Faculty of Science, National University of Singapore, 119260 Singapore<sup>b</sup> Institute of Materials Research and Engineering, Faculty of Science, National University of Singapore, 119260 Singapore<sup>c</sup> Department of Physics, Faculty of Science, National University of Singapore, 119260 Singapore

Received 30 March 2001; accepted 14 April 2001

## Abstract

Ultrafine lead titanate ( $\text{PbTiO}_3$ ) powders in tetragonal form have been successfully prepared via two processing routes, namely, conventional coprecipitation (CPC) and microemulsion-refined coprecipitation (MCP). The formation process of lead titanate from the resulting precursors was monitored using techniques such as thermal analyses, FTIR spectroscopy, Raman scattering spectroscopy and X-ray diffraction for the phase identification. It was found that the microemulsion-refined processing route led to a lower formation temperature for lead titanate than that observed in the conventional coprecipitation route, and there is no detectable pyrochlore phase during the formation of  $\text{PbTiO}_3$  in the former case. The two  $\text{PbTiO}_3$  powders have also been comparatively studied in particle morphology and specific surface areas. It indicates that the microemulsion-refined coprecipitation is the technique that results in the formation of the finer powder of lead titanate than the conventional coprecipitation does in the present work. © 2002 Elsevier Science B.V. All rights reserved.

**Keywords:** Lead titanate; Microemulsions; Ultrafine powder; Coprecipitation; FTIR and Raman spectra

## 1. Introduction

Lead titanate ( $\text{PbTiO}_3$ ), which exhibits a perovskite structure and a Curie temperature of 490 °C, belongs to the most important ferroelectric and piezoelectric families [1]. It has many important technological applications in electronics and microelectronics, because of its high Curie temperature, high pyroelectric coefficient and high spontaneous polarisation [2,3]. There are at least two incentives in preparing an ultrafine lead titanate powder, prefer-

ably in the range of nanometers: (i) to lower the ferroelectric phase transformation temperature [4]; and (ii) to improve the sintering behaviour of this material [5]. For this, a number of chemistry-based processing routes have been employed, including sol-gel synthesis [6–11], hydrothermal reactions [12–18], coprecipitation [19–23], molten salt preparation [24], solvothermal synthesis [25], polymerized complex [26] and emulsion technique [27]. The degree of success of these techniques in preparing an ultrafine lead titanate powder varies considerably from one to another.

Inverse microemulsion technique has been successfully used to prepare a range of ultrafine powders, including oxides [28,29], carbonates [30], silver chloride and bromide [31,32], high-temperature

\* Corresponding author. Advanced Materials Research Institute, SC2015, University of New Orleans, New Orleans, LA 70148, USA Fax: +1-504-280-3185.

E-mail address: jfang1@uno.edu (J. Fang).

$\text{YBa}_2\text{Cu}_3\text{O}_{7-x}$  superconductor [33,34], ceramic hydroxyapatite [35],  $\gamma\text{-Fe}_2\text{O}_3$  [36] and complex perovskite compounds [37]. During the inverse microemulsion processing, precursor particles are formed in the nanometer-sized aqueous domains surrounded by oil phase, and their sizes are therefore limited in the range of nanometers [32,35,37]. This isotropic dispersion of nanometer-sized aqueous droplets in microemulsions may well restrict the particle growth of  $\text{PbTiO}_3$  precursors when the precipitation/coprecipitation is effected in such synthetic medium, and makes the formation temperature for  $\text{PbTiO}_3$  significantly lowered due to the homogeneity of the resulting  $\text{PbTiO}_3$  precursors. Although  $\text{PbTiO}_3$  powders have been synthesized via various chemical processes, there have been little reports of applying an inverse microemulsion technique to this synthetic task. The objective of the present work is to investigate the phase development of  $\text{PbTiO}_3$  from microemulsion-derived precursor, in close comparison with that from conventional coprecipitated precursor.

## 2. Experimental procedures

### 2.1. Starting materials

The starting materials used in the present investigation included lead(II) nitrate (> 99.7% in purity, J.T. Baker, USA), titanium (IV) chloride (> 99.0% in purity, Hayashi Pure Chemical Industries, Japan), ammonia solution (concentration: 28.0–30.0 wt.%, J.T. Baker), a high-purity nitric acid (Hetalab Chemical, USA), a high-purity cyclohexane (Ajax Chemicals, Australia) and mixed poly(oxyethylene)<sub>5</sub> nonyl phenol ether (NP5) and poly(oxyethylene)<sub>9</sub> nonyl phenol ether (NP9) (in weight ratio: 2:1, Albright and Wilson Asia, Singapore).

### 2.2. Preparation of aqueous solution containing 0.30 M $[\text{TiO}(\text{NO}_3)_2\text{-Pb}(\text{NO}_3)_2]$

Aqueous solution of titanium oxynitrate was prepared by following the procedures of Yamamura et al. [38,39]. Weighed titanium tetrachloride ( $\text{TiCl}_4$ ) was dissolved in an appropriate amount of deionized water at ice-bath temperature. Cold ammonia solu-

tion (12 wt.%) was then added into the solution, resulting in the formation of titanium hydroxide hydrate. The gelatinous precipitates were filtered and washed repeatedly using deionized water until the pH of filtrate was close to 7.0, in order to remove chloride ions. Titanium oxynitrate in aqueous solution was prepared by dissolving the white precipitates in an appropriate amount of 3.0 M  $\text{HNO}_3$ , immediately followed by the concentration determination of  $\text{Ti}^{4+}$  using inductively coupled plasma (ICP, Thermo Jarrell Ash, IRIS/AP). The concentration of  $\text{TiO}(\text{NO}_3)_2$  was then adjusted to 0.30 M by adding an appropriate amount of deionized water. To prepare the aqueous solution containing 0.30 M  $[\text{Pb}(\text{NO}_3)_2\text{-TiO}(\text{NO}_3)_2]$  at equimolar ratio of  $\text{Pb}^{2+}/\text{Ti}^{4+}$ , an appropriate amount of lead nitrate was dissolved into the aqueous solution of titanium oxynitrate.

### 2.3. Preparation of $\text{PbTiO}_3$ powders

$\text{PbTiO}_3$  powders were prepared via two processing routes, namely conventional coprecipitation (hereafter CPC) and microemulsion-refined coprecipitation (hereafter MCP). In the CPC route, an aqueous solution containing 0.30 M  $[\text{Pb}(\text{NO}_3)_2\text{-TiO}(\text{NO}_3)_2]$  was titrated into a 12 wt.% ammonia solution in a beaker while being vigorously agitated using a mechanical stirrer. The precipitates were recovered by centrifugation and washed repeatedly using deionized water, followed by drying at 140 °C in an oven. In the MCP route, two microemulsion systems consisting of two common components, i.e. 56.0 wt.% cyclohexane and 24.0 wt.% NP5 + NP9 and differing only in aqueous phase, were prepared. The aqueous phase for one of the systems was 20.0 wt.% of 0.30 M  $[\text{Pb}(\text{NO}_3)_2\text{-TiO}(\text{NO}_3)_2]$ , while 20.0 wt.% of 2.85 M ammonia solution for the other. They were then mixed together by vigorous stirring for more than 20 min. The resulting precursor was retrieved by washing away the oil and surfactant using distilled ethanol, followed by centrifugal recovery and drying at 140 °C for 12 h.

### 2.4. Powder characterization

The as-dried precursors were characterized using thermogravimetric analysis (TGA) and differential

thermal analysis (DTA) (Dupont Instruments) at a heating rate of 10 °C/min in air from room temperature up to 900 °C. They were subsequently calcined in air at various temperatures, up to 800 °C, for 1 h, followed by phase analysis using X-ray diffractometer (CuK $\alpha$ , Philips PW1729), FTIR spectrometer (FTS135, Bio-Rad Laboratories) and Raman scattering spectrometer (Ramascope 2000). Transmission electron microscope (JEOL, 100CX) and scanning electron microscope (Philips, XL30) were also employed to analyze the particle morphology.

### 3. Results and discussion

#### 3.1. Thermal analysis of precursors

Figs. 1(a,b) and 2(a,b) are the TGA curves and DTA curves of PbTiO<sub>3</sub> precursors prepared via the both processing routes, respectively. The precursor prepared via the CPC route demonstrates a two-stage weight loss, a steady weight loss over the temperature range from room temperature to 200 °C, and a

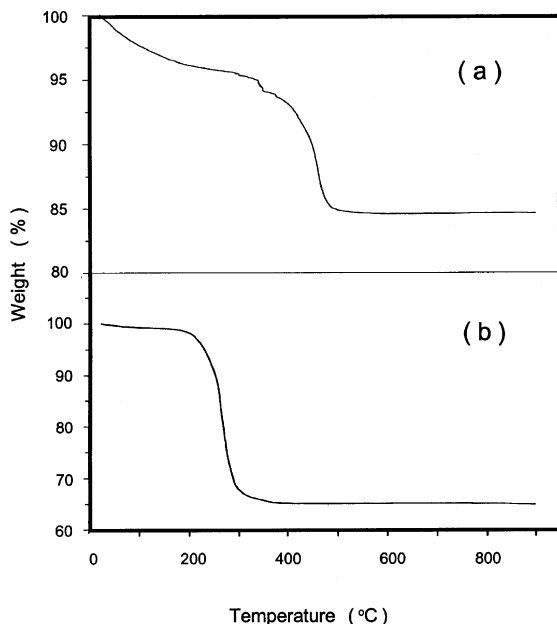


Fig. 1. TGA traces for the precursors prepared via (a) direct coprecipitation and (b) coprecipitation in microemulsions.

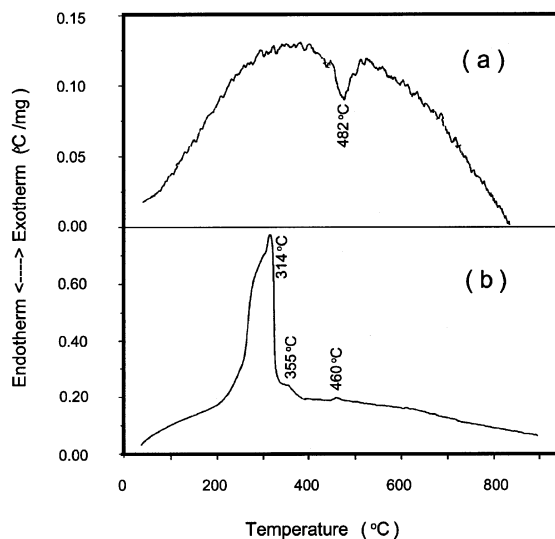


Fig. 2. DTA traces for the precursors prepared via (a) direct coprecipitation and (b) coprecipitation in microemulsions.

sharp fall in specimen weight over the temperature ranging from 350 to 460 °C. Little further weight loss is observed at temperatures above 500 °C, indicating the completion of all the reactions involving a weight loss. The weight loss at temperatures below 200 °C is believed to be due to the elimination of residual water and the dehydration of hydroxide hydrates in the precursors [14,40]. The fall in specimen weight over the temperature range from 350 to 460 °C is related to the decomposition of lead hydroxide and titanyl hydroxides. As shown in Fig. 3(a), this corresponds to a broadened endothermic reaction over the wide temperature range from 250 to 460°C in DTA trace of the precursor. Fig. 1(b) shows that the precursor prepared via the MCP route exhibits little weight loss over the temperature range from room temperature to 200 °C. However, there is a significant weight loss occurring over the temperature range from 230 to 300 °C. As shown in Fig. 2(b), there is a large exothermic peak at 314 °C with a large shoulder on the left-hand side. It may therefore be regarded as an overlap between two exotherms occurring over the very narrow temperature range. As will be discussed later, the shoulder is due to the decomposition of lead oxide and titanyl

hydroxide hydrates, together with the elimination of residual oil and surfactant phases from the precursor. The sharp exothermic peak is related to the formation of  $\text{PbTiO}_3$  as a result of the solid state reaction between nanocrystallites of  $\text{PbO}$  and  $\text{TiO}_2$ . There are two noticeable exotherms peaking at 355 and 460 °C, respectively. They are believed to be due to the crystallization of remaining  $\text{PbO}$  and the subsequent conversion to  $\text{PbTiO}_3$ .

### 3.2. X-ray diffraction

To further study the phase development with increasing calcination temperature in each of the two precursors, they were calcined for 1 h in air at various temperatures, up to 800 °C, followed by phase analysis using XRD. Figs. 3 and 4 are the XRD traces at various calcination temperatures for the precursors prepared via the CPC and MCP routes, respectively. In the coprecipitated precursor, little  $\text{PbTiO}_3$  crystalline phase was developed accompanying with red-PbO characterized by a group of peaks centered around  $2\theta = 28.7^\circ$  and  $54.9^\circ$  when it was calcined at 400 °C. Heating up to 450 °C led to an increasing development of tetragonal  $\text{PbTiO}_3$ , mixing with red-PbO represented by the characteristic peak at  $2\theta = 28.74^\circ$ , yellow-PbO by the characteristic peak at  $2\theta = 29.09^\circ$ , and a small amount of anatase  $\text{TiO}_2$  by the characteristic peak at  $2\theta = 25.28^\circ$ . With increasing calcination temperature to 500 °C, the amount of  $\text{PbTiO}_3$  phase increased at the expenses of non- $\text{PbTiO}_3$  phases including red-PbO, yellow-PbO and anatase  $\text{TiO}_2$  ( $2\theta = 25.28^\circ$  and  $48.05^\circ$ ) phases. At this temperature, a certain amount of pyrochlore phase was also formed as identified by the characteristic peaks [9,41]. Calcination at 600 °C resulted in a further development of  $\text{PbTiO}_3$  phase and most of intermediate phases were eliminated. In particular, the peak corresponding to yellow-PbO ( $2\theta = 29.09^\circ$ ) was intensified and the peak corresponding to red-PbO ( $2\theta = 28.74^\circ$ ) had vanished, revealing that  $\text{PbO}$  as intermediate phase has completely converted to yellow-PbO phase at 600 °C. Red-PbO exhibits a tetragonal structure and yellow-PbO exhibits an orthorhombic structure. It is known that the former is stable at room temperature and the latter is at stable form above 488 °C under normal

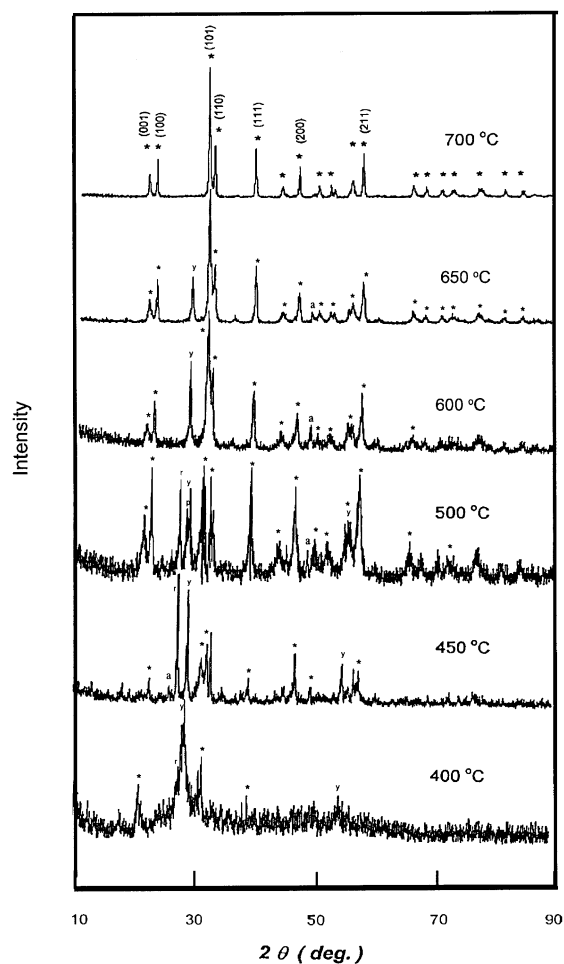


Fig. 3. XRD traces of the directly coprecipitated  $\text{PbTiO}_3$  powders, calcined for 1 h at 400, 450, 500, 600, 650 and 700 °C, respectively. (\* tetragonal  $\text{PbTiO}_3$ ; p, pyrochlore phase; y, yellow  $\text{PbO}$ ; r, red- $\text{PbO}$ ; a, anatase  $\text{TiO}_2$ .)

pressure condition. However, the transformation temperature between both is sensitive to impurities and certain doping elements [42]. Further increasing the calcination temperature to 650 °C led a reduction in the amount of yellow-PbO, and a single-phase  $\text{PbTiO}_3$  powder is obtained when the precursor is calcined at temperatures above 700 °C. At 700 °C, no rutile  $\text{TiO}_2$  was detected as an intermediate phase. As shown in Fig. 4, a noticeable amount of fine  $\text{PbTiO}_3$  crystallites are developed in the MCP precursor at a calcination temperature of as low as 350 °C, although crystalline yellow-PbO phase dominates

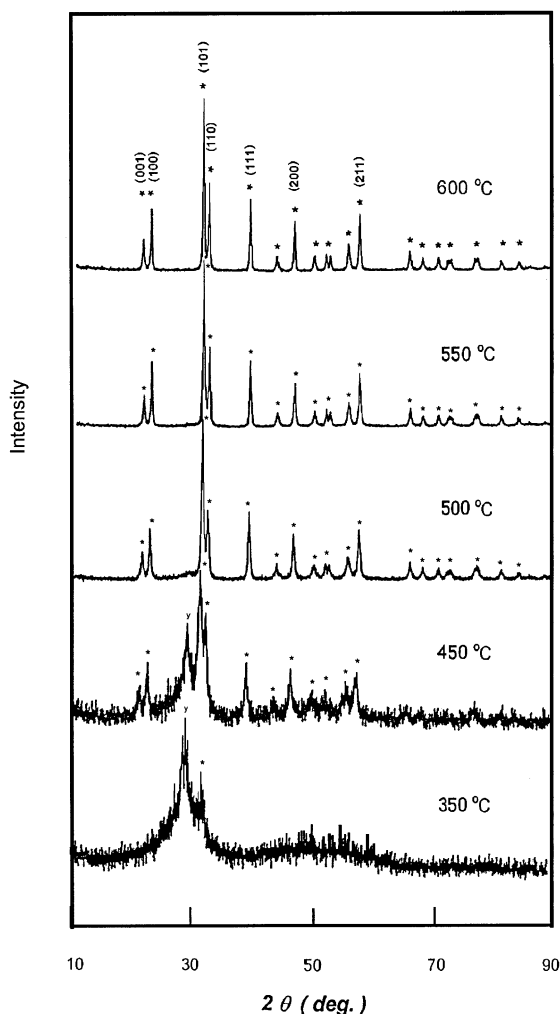


Fig. 4. XRD traces of the  $\text{PbTiO}_3$  powders prepared via the route of coprecipitation in microemulsions and calcined at for 1 h at 350, 450, 500, 550 and 600 °C, respectively. (\* tetragonal  $\text{PbTiO}_3$ ; y, yellow  $\text{PbO}$ .)

the XRD trace. Tetragonal  $\text{PbTiO}_3$  becomes the predominant phase at 450 °C, and it is the only XRD detectable phase in the precursor when calcined at 500 °C. There was no pyrochlore phase observed during the calcination process in the precursor derived via the MCP route. It is seen from Fig. 4 that the increase of calcination temperature ranging from 350 to 450 °C does not result in very much increase in the crystallinity of yellow-PbO. Instead, the yellow-PbO reacts with amorphous  $\text{TiO}_2$  to form

$\text{PbTiO}_3$ . The MCP-precursor demonstrates lower formation temperature for tetragonal  $\text{PbTiO}_3$  than the CPC-precursors does in the present work. Both crystalline red-PbO and crystalline  $\text{TiO}_2$  were not observed as intermediate phases on the basis of phase analysis using XRD. From the above descriptions, it is worth noting that in the precursor derived via the MCP route, the temperature of developing a crystalline  $\text{PbTiO}_3$  is as low as 350 °C. By far, it is much lower than those reported for most chemistry-based routes such as sol-gel technique. In sol-gel derived precursor, a pyrochlore phase was observed when it was calcined at below 500 °C [43], although  $\text{PbTiO}_3$  gel was crystallized at 500 °C [44]. Löbmann et. al. [8] reported that the transition from an amorphous phase to the tetragonal  $\text{PbTiO}_3$  phase occurred at temperatures between 500 and 600 °C when the an aerogel was prepared via a sol-gel process. In contrast, the formation temperature for a single tetragonal  $\text{PbTiO}_3$  phase in this work (MCP route) is 500 °C, which is lower than the reported formation temperature for a single perovskite  $\text{PbTiO}_3$  phase via many other chemistry-based processing routes. For example, a calcination temperature of ~ 900 °C was required for the formation of a single  $\text{PbTiO}_3$  phase in an emulsion-derived precursor, although tetragonal  $\text{PbTiO}_3$  crystallites were observed to form at 560 °C [27]. A similar calcination temperature was needed for the hydrolyzed precursor from alkoxides [6]. The calcination temperature required for the coprecipitated precursors was in the range of 700 to 800 °C [19,45,46], which is very similar to that observed in our CPC-derived precursor.

### 3.3. Raman and FTIR spectra

To confirm the phase development for  $\text{PbTiO}_3$  as observed using XRD, both as-prepared  $\text{PbTiO}_3$  powders were characterized using a Raman spectrometer. By comparison with the typical Raman spectrum of  $\text{PbTiO}_3$  published in previous work [9,47], the formation of tetragonal  $\text{PbTiO}_3$  can be traced on both powders calcined at various temperatures in each processing route. Fig. 5 illustrates the Raman spectra for both  $\text{PbTiO}_3$  powders recorded at room temperature. Both  $\text{PbTiO}_3$  powders (derived from CPC and MCP) calcined at low temperatures only showed fluorescence bands due to organic residuals. How-

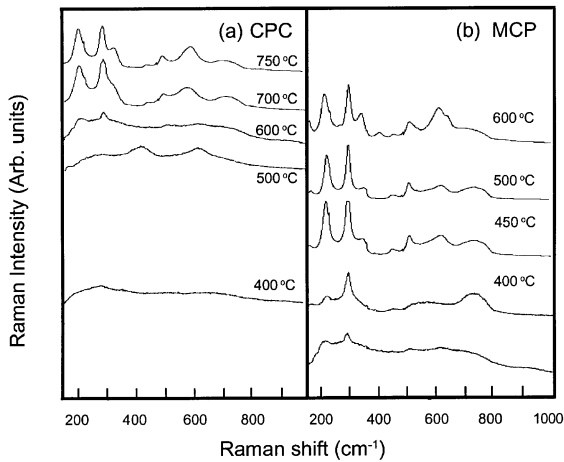


Fig. 5. Raman spectra of  $\text{PbTiO}_3$  powders derived from (a) CPC and (b) MCP routes after various stages of heat treatment.

ever, the crystallization temperature for  $\text{PbTiO}_3$  is different between two routes. In CPC route, the initial crystallization of  $\text{PbTiO}_3$  can only be ob-

served from a spectrum obtained from the powder calcined at 600 °C and a well developed tetragonal spectrum can be detected at 700 °C. In contrast, the presence of  $\text{PbTiO}_3$  was indicated when the precursor derived via MCP route was calcined at 350 °C. A distinct tetragonal  $\text{PbTiO}_3$  Raman spectrum [47] was obtained when the calcination temperature was raised to 400 °C. On the basis of the Raman spectroscopic investigation, it may be concluded that tetragonal  $\text{PbTiO}_3$  was formed at 600 and 400 °C for the precursors derived via CPC and MCP routes, respectively. In principle, this is in agreement with the results obtained using XRD phase analysis. However, it is difficult to observe the phase development at low temperatures using Raman technique. In order to understand the processes at low temperatures in both precursors derived via the CPC and MCP routes, it is necessary to conduct an FTIR study as a supplemental investigation.

Fig. 6(a,b) illustrate the FTIR spectra for both powders derived via the CPC and MCP routes and

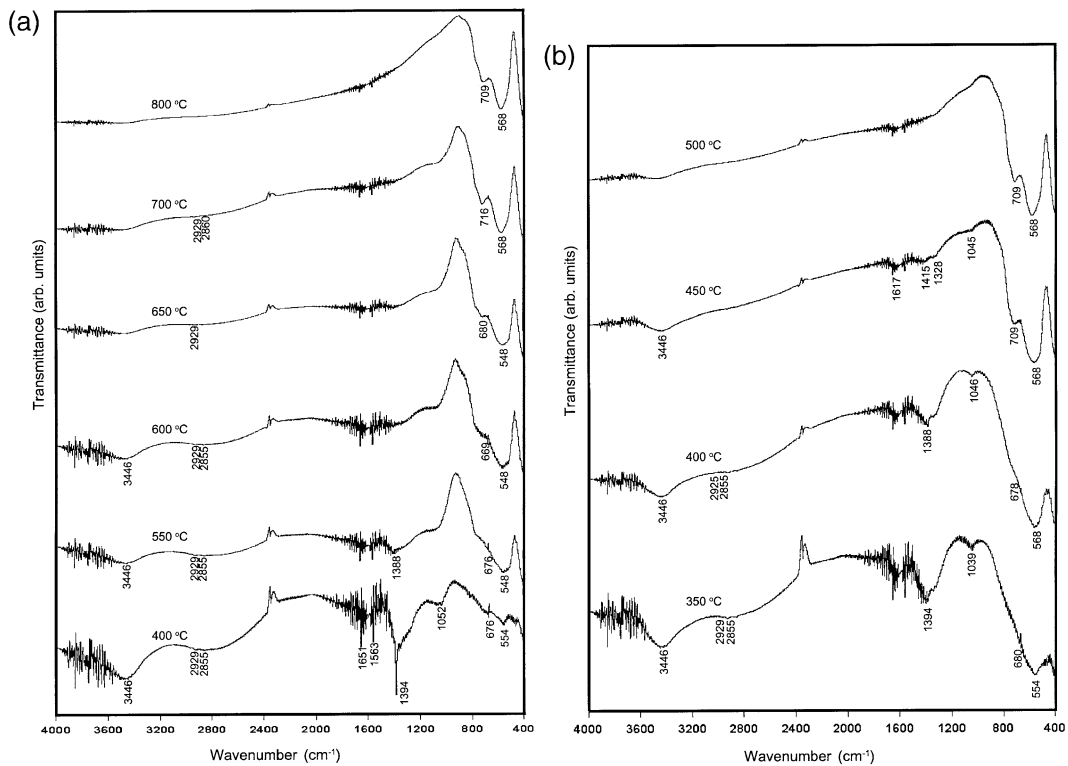


Fig. 6. (a) IR spectra of  $\text{PbTiO}_3$  powders prepared via the direct coprecipitation route and calcined for 1 h at various temperatures; (b) IR spectra of the  $\text{PbTiO}_3$  powders coprecipitated in microemulsions and calcined for 1 h at various temperatures.

calcined at various temperatures. For comparison, the IR spectra of PbO were recorded as standard references using commercial PbO powders with high purity, exhibiting a strong characteristic absorption band at  $\sim 1394\text{ cm}^{-1}$ , together with other absorption bands at 678 and  $460\text{ cm}^{-1}$ . The IR spectrum for CPC-derived powder calcined at  $400\text{ }^\circ\text{C}$  in Fig. 6(a) clearly indicates the presence of anatase  $\text{TiO}_2$  characterized by the absorption bands at 554, 676, 2855, 2929 and  $3446\text{ cm}^{-1}$ . These bands coincide well with the characteristic wave numbers of anatase  $\text{TiO}_2$  [48]. The strong absorption at  $1394\text{ cm}^{-1}$  indicates the presence of PbO as a major phase. It was reported that absorption bands over the range of  $900\text{--}1700\text{ cm}^{-1}$  are mainly related to the organic groups [11]. Therefore, absorption bands at 1052, 1563 and  $1651\text{ cm}^{-1}$  are attributed to the organic residuals in the powder. Increasing the calcination temperature to  $550\text{ }^\circ\text{C}$  results in decrease in intensity of the organic and PbO absorption bands and the further enhancement of anatase  $\text{TiO}_2$  phase. The organic residuals were completely eliminated when the CPC-derived precursor was calcined at  $600\text{ }^\circ\text{C}$ , where the corresponding IR spectrum exhibits apparent bands from anatase  $\text{TiO}_2$  and a further decreased band of PbO.  $\text{PbTiO}_3$  started to form and the intermediate phase such as PbO and  $\text{TiO}_2$  became minor phases when the calcination temperature was further raised, as shown by the spectra of the powders calcined at 650 and  $700\text{ }^\circ\text{C}$ . Eventually, an IR spectrum corresponding to the single-phase  $\text{PbTiO}_3$  [49] was obtained when the precursor was calcined at  $800\text{ }^\circ\text{C}$ . Fig. 6(b) shows the IR spectra of MCP-derived precursors calcined at various temperatures. Based on these spectra, the powder calcined at  $350\text{ }^\circ\text{C}$  consisted of a mixture containing anatase  $\text{TiO}_2$ , PbO, and organic residuals as indicated by the band group of 554, 680, 2855, 2929,  $3446\text{ cm}^{-1}$ , band at  $1394\text{ cm}^{-1}$  and band at  $1039\text{ cm}^{-1}$  [11,48]. Heating up to  $400\text{ }^\circ\text{C}$  led to an enhancement in the intensity for anatase  $\text{TiO}_2$  and a rapid decrease in intensity of the absorption band for PbO, together with a decrease in intensity for organic residuals. The spectrum for the powder calcined at  $450\text{ }^\circ\text{C}$  indicates the vanishing of anatase  $\text{TiO}_2$  bands and a further reduction in the intensity related to the organic residuals. It also demonstrates an apparent formation of  $\text{PbTiO}_3$  phase. An IR spectrum corresponding to well developed

single-phase  $\text{PbTiO}_3$  was obtained when the precursor was calcined at  $500\text{ }^\circ\text{C}$ . This is in close agreement with what has been revealed by phase analysis using XRD technique.

### 3.4. Morphology of $\text{PbTiO}_3$ powders

The  $\text{PbTiO}_3$  powders prepared via both processing routes are different in particle/agglomerate size and morphology. Figs. 7(a,b) are two SEM micrographs showing the microstructure of both powders. Both of them were calcined at  $600\text{ }^\circ\text{C}$  for 1 h. The CPC-derived  $\text{PbTiO}_3$  powder consists of primary particles of micrometers in size. In contrast, discrete particles of  $\sim 100\text{ nm}$  are observed in the powder via MCP route, together with a more or less rounded particle morphology. Fig. 8 is a TEM micrograph

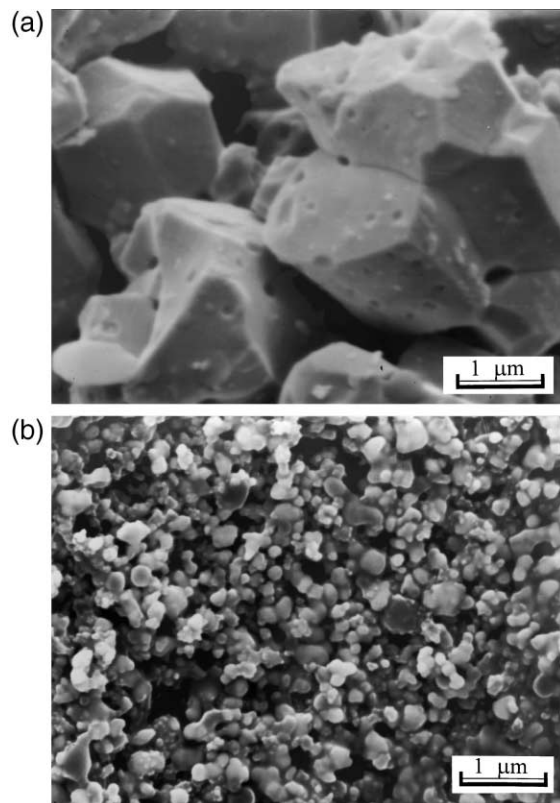


Fig. 7. SEM micrographs showing the microstructure of  $\text{PbTiO}_3$  powders prepared via (a) direct coprecipitation and (b) coprecipitation in microemulsions. All the three powders were calcined at  $600\text{ }^\circ\text{C}$  for 1 h, followed by treatment in 5 wt.% acetic acid.

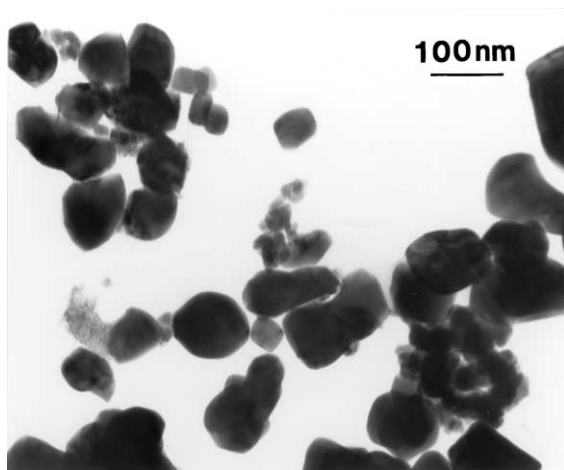


Fig. 8. A TEM micrograph showing the microstructure of  $\text{PbTiO}_3$  powder prepared via the coprecipitation in microemulsions route (powder was calcined at  $600\text{ }^\circ\text{C}$  for 1 h).

further showing the ultrafine particle characteristics for the powder derived via the MCP route.

#### 4. Conclusions

$\text{PbTiO}_3$  powders in tetragonal form have been prepared via two processing routes: CPC and MCP. Precursors derived from these two processing routes exhibit very different formation temperature for tetragonal  $\text{PbTiO}_3$  phase. On the basis of XRD phase analysis, the directly coprecipitated precursor requires calcination at  $700\text{ }^\circ\text{C}$  for 1 h, in order to develop a single-phase  $\text{PbTiO}_3$  powder. This is in contrast to  $500\text{ }^\circ\text{C}$  for 1 h required by the precursors derived via the MCP routes. Studies of Raman/FTIR spectra indicate that tetragonal  $\text{PbTiO}_3$  phase was formed at  $600/800\text{ }^\circ\text{C}$  and  $400/500\text{ }^\circ\text{C}$  in two precursors, respectively. With increasing calcination temperature, the precursors derived from CPC route was first decomposed into crystalline  $\text{PbO}$  and anatase  $\text{TiO}_2$  phases as intermediates; these oxides then react with each other to form  $\text{PbTiO}_3$  by further increasing the calcination temperature. Unlike what is being observed in CPC-derived precursor, no pyrochlore phase was detected as an intermediate phase when the MCP-derived precursor was calcined. In addition, the microemulsion processing routes also

results in the formation of finer  $\text{PbTiO}_3$  powders than that prepared via the conventional coprecipitation route, as observed using SEM for the powders calcined at  $600\text{ }^\circ\text{C}$  for 1 h.

#### Acknowledgements

This work was supported by research grants RP950613 and RP950605 from the National University of Singapore.

#### References

- [1] C. Chandler, C. Roger, M. Hampden-Smith, *Chem. Rev.* 93 (1993) 1205.
- [2] W.C. Hendricks, S.B. Desu, C.H. Peng, *Chem. Mater.* 6 (1994) 1955.
- [3] J.S. Wright, L.F. Francis, *J. Mater. Res.* 8 (1993) 1712.
- [4] K. Ishikawa, N. Okada, K. Takada, T. Nomura, M. Hagino, *Jpn. J. Appl. Phys.* 33 (1994) 3495.
- [5] L.M. Levinson, *Electronic Ceramics*, Marcel Dekker, New York, 1988, p. 209.
- [6] S. Kim, M.-C. Jun, S.-C. Hwang, *J. Am. Ceram. Soc.* 82 (1999) 289.
- [7] Q.F. Zhou, J.X. Zhang, H.L.W. Chan, C.L. Choy, *Ferroelectrics* 1995 (1997) 211.
- [8] P. Löbmann, W. Glaubbitt, J. Fricke, *J. Am. Ceram. Soc.* 80 (1997) 2658.
- [9] D. Bersani, P.P. Lottici, A. Montenero, S. Pignoni, G. Gnappi, *J. Mater. Sci.* 31 (1996) 3153.
- [10] P. Löbmann, W. Glaubbitt, J. Gross, J. Fricke, *J. Non-Cryst. Solids* 186 (1995) 59.
- [11] L. Lan, A. Montenero, G. Gnappi, E. Dradi, *J. Mater. Res.* 30 (1995) 3137.
- [12] J. Moon, T. Li, C.A. Randall, J.H. Adair, *J. Mater. Res.* 12 (1997) 189.
- [13] H. Cheng, J. Ma, Z. Zhao, L. Qi, *J. Mater. Sci. Lett.* 15 (1996) 1245.
- [14] Y. Ohara, K. Koumoto, T. Shimizu, H. Yanagida, *J. Mater. Sci.* 30 (1995) 263.
- [15] S. Sato, T. Murakata, H. Yanagi, F. Miyasaka, *J. Mater. Sci.* 29 (1994) 5657.
- [16] K. Kikuta, A. Tosa, T. Yogo, S. Hirano, *Chem. Lett.* (1994) 2267.
- [17] C.H. Lin, S.C. Pei, T.S. Chin, T.P. Wu, *Ceram. Trans.* 30 (1993) 261.
- [18] H. Cheng, J. Ma, Z. Zhao, D. Qiang, Y. Li, X. Yao, *J. Am. Ceram. Soc.* 75 (1992) 1123.
- [19] G.R. Fox, E. Breval, R.E. Newnham, *J. Mater. Sci.* 26 (1991) 2566.

- [20] G.R. Fox, J.H. Adair, R.E. Newnham, *J. Mater. Sci.* 25 (1990) 3634.
- [21] M.H. Lee, A. Halliyal, R.E. Newnham, *J. Am. Ceram. Soc.* 72 (1989) 986.
- [22] G. Marbach, S. Stotz, M. Klee, J.W.C. de Vaies, *Physica C* 161 (1989) 111.
- [23] J. Hagberg, R. Rautioaho, J. Levoska, A. Uusimaki, T. Murtoniemi, T. Kokkmaki, S. Leppavuori, *Physica C* 160 (1989) 369.
- [24] H. Idrissi, A. Aboujalil, B. Durand, *J. Eur. Ceram. Soc.* 19 (1999) 1997.
- [25] D.R. Chen, R.R. Xu, *J. Mater. Chem.* 8 (1998) 965.
- [26] M. Kakihana, T. Okuho, M. Arima, O. Uchiyama, M. Yashima, M. Yoshimura, Y. Nakamuya, *Chem. Mater.* 9 (1997) 451.
- [27] C. Lu, Y. Xu, *Mater. Lett.* 27 (1996) 13.
- [28] S. Hingorani, D.O. Shah, M.S. Multani, *J. Mater. Res.* 10 (1995) 461.
- [29] M. Gobe, K. Kon-no, K. Kandori, A. Kitahara, *J. Colloid Interface Sci.* 93 (1983) 293.
- [30] K. Kandori, K. Kon-no, A. Kitahara, *J. Colloid Interface Sci.* 115 (1987) 579.
- [31] M.J. Hou, D.O. Shah, in: Y.A. Attia, B.M. Moudgil, S. Chander (Eds.), *Interfacial Phenomena in Biotechnology and Materials Processing*, Elsevier, Amsterdam, 1988, p. 443.
- [32] C.H. Chew, L.M. Gan, D.O. Shah, *J. Dispersion Sci. Technol.* 11 (1990) 593.
- [33] P. Ayyub, M.S. Multrani, *Mater. Lett.* 10 (1991) 431.
- [34] P. Ayyub, A.N. Maitra, D.O. Shah, *Physica C* 168 (1990) 571.
- [35] G.K. Lim, J. Wang, S.C. Ng, L.M. Gan, *Mater. Lett.* 28 (1996) 431.
- [36] V. Chhabra, P. Ayyub, S. Chattopadhyay, A.N. Maitra, *Mater. Lett.* 26 (1996) 21.
- [37] L.M. Gan, H.S.O. Chan, L.H. Zhang, C.H. Chew, B.H. Loo, *Mater. Chem. Phys.* 27 (1994) 263.
- [38] H. Yamamura, S. Kuramoto, H. Haneda, A. Watanabe, S. Shirasaki, *Yogyo Kyokaishi* 94 (1986) 470.
- [39] H. Yamamura, A. Watanabe, S. Shirasaki, Y. Moriyoshi, M. Tanada, *Ceram. Int.* 11 (1985) 17.
- [40] D.L. Perry, S.L. Phillips (Eds.), *Handbook of Inorganic Compounds*, CRC Press, Boca Raton, 1995, p. 216.
- [41] Y. Takahashi, K. Yamaguchi, *J. Mater. Sci.* 25 (1990) 3950.
- [42] J.C. Bailar Jr., H.J. Emelús, R. Hyholm, A.F. Trotman-Dickenson (Eds.), *Comprehensive Inorganic Chemistry*, vol. 2, 1973, p. 119, Oxford.
- [43] G. Antonioli, D. Bersani, P.P. Lottici, I. Manzini, S. Bassi, G. Gnappi, A. Montenero, *J. Physiqueiv* 7 (1997) 1161 (part 2).
- [44] Y. Chen, H.L.W. Chan, C.L. Choy, *J. Am. Ceram. Soc.* 81 (1998) 1231.
- [45] J.B. Blum, S.R. Gurkovich, *J. Mater. Res.* 20 (1985) 4479.
- [46] C.M. Jimenez, G.F. Arroyo, L.D.O. Guillen, in: P. Vincenzini (Ed.), *Ceramic Powders*, Elsevier, Amsterdam, 1983, p. 564.
- [47] S. Li, R.A. Condrate Sr., R.M. Spriggs, *Spectrosc. Lett.* 21 (9/10) (1988) 969.
- [48] R.A. Nyquist, R.O. Kagel, *The Handbook of Infrared and Raman Spectra of Inorganic Compounds and Organic Salts*, vol. 3, Academic Press, San Diego, 1997, p. 102.
- [49] R.A. Nyquist, R.O. Kagel, *The Handbook of Infrared and Raman Spectra of Inorganic Compounds and Organic Salts*, vol. 4, Academic Press, San Diego, 1997, p. 104.